ACS OMEGA

http://pubs.acs.org/journal/acsodf

Article

Generation and Use of Lignin-*g*-AMPS in Extended DLVO Theory for Evaluating the Flocculation of Colloidal Particles

Yanzhu Guo, Fangong Kong, and Pedram Fatehi*

Cite This: *ACS Omega* 2020, 5, 21032−21041

Read Online

ACCESS | Metrics & More | Article Recommendations

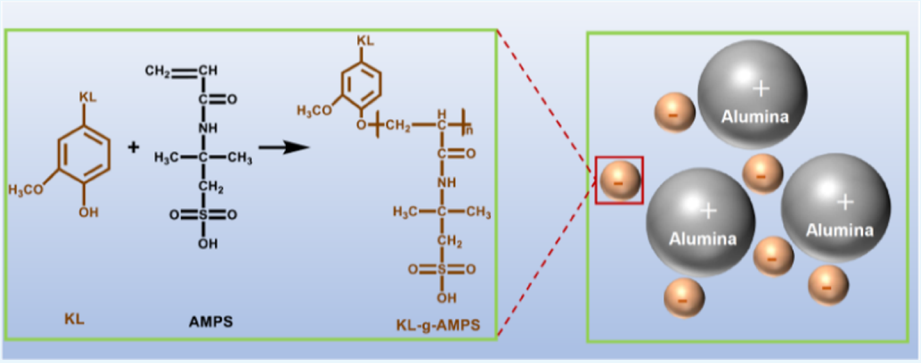

ABSTRACT: In this work, Kraft lignin (KL) was polymerized with 2-acrylamido-2-methylpropane sulfonic acid (AMPS) to generate an anionic water-soluble KL-*g*-AMPS polymer. The effects of reaction conditions on the charge density of polymers were evaluated to induce lignin-based polymers with the highest anionic charge density. The optimal process conditions were 2.5 mol/mol AMPS/lignin, 0.6 g/g solid/water ratio, 2.0 initiator/lignin weight ratio, 80 °C, 120 min, and pH 1.5, which yielded KL-*g*-AMPS with the anionic charge density of 4.28 mequiv/g and the grafting ratio of 285%. The chemical structure and compositions of the polymers were confirmed by ^{1}H NMR and elemental analysis. The flocculation performance of the polymer was evaluated in an aluminum oxide suspension, and its performance was compared with that of a homopolymer of AMPS produced under the same conditions. In addition, the extended Derjaguin−Landau−Verwey−Overbeek (XDLVO) theory was applied to study the flocculation mechanism of the polymers and alumina particles. The results revealed that electrostatic interaction was found to be the dominant force in this flocculation process.

INTRODUCTION

Owing to its cost-effectiveness and ease of operation, flocculation is the most commonly used technique to achieve an efficient solid−liquid separation in many industrial processes,[1] such as coal mining and mineral processes,[2] wastewater treatment,[3−5] pulp and paper processes,[6] and biotechnology operations.[7] In these processes, flocculants are essential elements to destabilize suspended colloids. The currently used flocculants in the industry are mainly synthetic organic polymers, e.g., polyacrylamide (PAM) and its derivatives.[8] However, these flocculants and their derivatives can cause environmental issues because they possess some unfavorable properties, e.g., non-biodegradability and hazardousness to humans.[9] Therefore, efforts have been made on combining synthetic and natural polymers to create more environmentally friendly flocculants.

Lignin is renewable biomass composed of methoxylated phenylpropane structures, and it can be widely used as a raw material of seminatural products, such as flocculants.[10] In the past, various lignin-based polymers were produced for this purpose. For example, a variety of vinyl monomers, e.g., acrylamide, acrylic acid,[11,12] dimethyl diallyl ammonium chloride,[13,14] 2-(methacryloyloxy)ethyl trimethylammonium chloride (METAC),[15] have been successfully polymerized onto lignin. In this context, 2-acrylamido-2-methylpropane sulfonic acid (AMPS) is a multigroup anionic amide monomer.[16] Its strong anionic nature, solubility, and good salt-resistance result from the presence of sulfonic groups on its structure.[17] Additionally, AMPS-based polymers were reported to have more resistance against hydrolysis and acid/base environment.[18,19] These properties make AMPS an ideal candidate for flocculant production. To the best knowledge of

Received: June 1, 2020
Accepted: July 23, 2020
Published: August 11, 2020

the authors of this work, the polymerization of lignin and AMPS to generate KL-*g*-AMPS and the use of the produced polymer as a flocculant has not been reported in the past. The first objective of this work was to evaluate this polymerization reaction.

Charge neutralization, polymer bridging, and electrostatic patch have been described as the primary mechanisms of flocculation processes.[1,20,21] It is widely accepted that polymeric flocculants develop flocs with different properties when adsorbed onto particles.[22] Hydrodynamic and short-range interactions are considered to be the major factors for the collision of flocculants and particles.[23] These interactions can bring two particles into close vicinity of each other.[24] The chance of the two particles colliding and forming flocs depends on the short-range interactive forces.[25] It has been reported that these interactions are essentially related to the electrical nature, attractive (generally van der Waals forces), repulsive (electrical double layers), and Lewis acid−base interaction (hydrophobic interaction) in the colloidal systems.[26] These interfacial interactions between two surfaces can be generally described following the extended Derjaguin−Landau−Verwey−Overbeek (XDLVO) theory,[27] which has been developed to explain the flocculation of algal to clays[23] and the adsorption of nanosized particles to the surface of bacteria[28] or calcite,[29] for instance. The second objective of this study was to investigate the role of interfacial interactions between KL-*g*-AMPS polymer and alumina particles following the fundamentals of the XDLVO theory. Aluminum oxide particles were chosen as the model clays in this study, as they are widely used in ceramic and mineral processes due to their high thermal resistance and strength.[22] Commonly, the wastewaters produced in these processes contain large amounts of aluminum oxide particles that possess positive charges on their surfaces and cause high water turbidity. Anionic flocculants are effective in separating the aluminum oxide particles from the colloidal suspension.[30] Therefore, the prepared KL-AMPS flocculants could be used in the wastewater treatment of mineral or ceramic industries. The main novelties of this work were (1) the development of a green flocculant to replace oil-based ones and (2) the understanding of the interfacial interactions between flocculants and aluminum oxide particles.

EXPERIMENTAL METHODOLOGY

Materials. Softwood Kraft lignin (KL) was produced via the pilot plant facilities of FPInnovations in Thunder Bay, ON, Canada. Also, 2-acrylamido-2-methylpropane sulfonic acid (AMPS) with 99% purity, $K_2S_2O_8$, $NaNO_3$, KCl, NaOH with 97% purity, deuterium oxide (D_2O), aluminum oxide particles, poly (ethylene oxide), glycerol, diiodomethane, poly(acrylic acid) (PAA), and trimethylsilyl propanoic acid (TPA), all of analytical grades, were purchased from Sigma-Aldrich Company. The dialysis membrane with a molecular weight cut off of 1000 g/mol was purchased from Spectrum-Labs.

Synthesis of KL-*g*-AMPS Polymers. In this set of experiments, 2 g of KL was dispersed in a certain amount (8.1−20.9 g) of water in a plastic bag. The desired amount (1.15−6.90 g) of AMPS was added to the mixture, and the pH was adjusted to the desired value (1.0−12.0). After purging with nitrogen for 5 min, 0.03 g of potassium persulfate was added to the mixture, which was then purged with nitrogen for another 10 min and placed into a water bath to start polymerization at different temperatures (50−90 °C) for 30−240 min. Every 15 min, the mixtures in the plastic bag were kneaded by hands for 2 min. After cooling to room temperature, the mixtures in the plastic were mixed with 150 mL of 80 vol % ethanol/water to precipitate the produced lignin-based polymer from the rest of the reaction mixtures.[31] The addition of ethanol to the mixtures converted the solution mixtures to suspensions. The suspensions were then centrifuged at 3500 rpm for 10 min (Sorvall ST 16 Laboratory Centrifuge, Thermo Fisher) and the obtained precipitates were collected and resuspended in 100 mL of 80 vol % ethanol/water, stirred at 300 rpm for 30 min, and centrifuged at 3500 rpm for 10 min. This procedure was repeated twice. After the collection of the lignin polymer product, it was dissolved in 100 mL of water, and the solution was neutralized by 1 mol/L NaOH and transferred into membrane dialysis tubes to dialyze against distilled water for 2 days. After drying the resultant solutions in a 105 °C oven, the purified polymers, KL-*g*-APMS, were collected. The homopolymer of PAMPS was produced following the same procedure under the conditions of 10 g of AMPS, 60% solid/water ratio, 2% initiator/lignin weight ratio, 80 °C, 120 min, and pH 1.5.

Characterization of KL, KL-*g*-AMPS, and PAMPS Samples. Approximately, 0.20 g of the polymers was dissolved in 20 g of water, and the solutions were immersed in a water bath shaker (Innova 3100, Brunswick Scientific, Edison, NJ) and shaken (150 rpm) at 30 °C for 2 h. The charge density of the polymer was then analyzed using a Particle Charge Detector (Mütek PCD 04) with 0.005 M poly(dimethyl diallyl ammonium chloride) solution as the standard titration solution.

The carbon, hydrogen, oxygen, nitrogen, and sulfur contents of KL, KL-*g*-AMPS, and PAMPS were determined using a Vario EL Cube Elemental Analyzer (Elementar, Germany). The samples were oven-dried in 105 °C oven for 12 h to remove any moisture before analysis. As KL lacked any nitrogen element in its chemical structure, the nitrogen content of KL-*g*-AMPS was derived from AMPS that was attached to KL. The grafting ratio of AMPS on KL was identified using eq 1 according to the nitrogen content of KL-*g*-AMPS polymers.[12]

$$\text{grafting ratio } (\%) = \frac{\text{N}/14 \times 229.25}{100 - \text{N}/14 \times 229.25} \times 100 \quad (1)$$

where N is the nitrogen content of the samples (wt %) and 14 and 229.25 are the molecular weights (g/mol) of nitrogen and AMPS sodium, respectively.

The molecular weights and their distributions for KL, KL-*g*-AMPS, and PAMPS samples were analyzed using gel permeation chromatography (GPC, Malvern, GPCmax VE2001 Module Viscotek TDA305), which was equipped with a refractive index (RI) detector and a series of aqueous columns including PolyAnalytic PAA206 and PAA203. The solution of 0.1 M $NaNO_3$ at the flow rate of 0.70 mL/min was used as an eluent, while poly(ethylene oxide) samples were employed as standards. The temperature of the columns was 35 °C. In this analysis, 20 mg of KL, KL-*g*-AMPS, and PAMPS samples were dissolved into 10 mL of 0.1 mol/L $NaNO_3$ solution by stirring at 400 rpm and room temperature for 24 h. After filtering the solution with a 0.2 μm nylon filter (13 mm diameter), the filtrates were injected into the GPC system for analysis.

The ^{1}H NMR spectra of KL, KL-*g*-AMPS, and PAMPS samples were collected using an INOVA-500 MHz instrument (Varian). In this analysis, 30 mg of samples were dissolved into

https://dx.doi.org/10.1021/acsomega.0c02598
ACS Omega 2020, 5, 21032−21041

1 mL of D_2O by stirring them at 200 rpm for 1 h, to which 0.025 g of TPA was added as the internal standard. The pulse angle of 45° and the relaxation time of 1.0 s were employed during nuclear magnetic resonance (NMR) analysis.

The ζ-potentials of KL, KL-*g*-AMPS, PAMPS, and aluminum oxide suspensions were measured by a ζ-potential analyzer (NanoBrook Omni, Brookhaven Instruments). The suspensions of KL, KL-*g*-AMPS, and PAMPS samples (1 g/L) at pH 7.0 were prepared by stirring them at 300 rpm for 30 min and then diluting them with 1 mM filtered KCl solution before the ζ-potential analysis. The suspensions of alumina were prepared for analysis by diluting 100 μL of aluminum oxide suspensions (5 g/L at pH 7.0) into 20 mL of filtered KCl solution.

According to a published procedure,[32] the hydrodynamic sizes of KL, KL-*g*-AMPS, PAMPS, and aluminum oxide particles were determined using a dynamic light scattering instrument (BI-200SM, Brookhaven Instruments), which was equipped with a solid-state laser (35 MW power). The laser was emitted at a scattering angle of 90° and a wavelength of 637 nm. The KL, KL-*g*-AMPS, PAMPS, and alumina particles at a 1 g/L aqueous concentration and pH 7.0 were prepared and stirred at 300 rpm and 25 °C for 24 h. The suspensions were filtered through a 0.45 μm syringe filter and put into the instrument, whose operation was carried out for 2 min. The analysis was repeated five times and then the mean values were calculated.

The contact angles of KL, KL-*g*-AMPS, PAMPS, and aluminum oxide were determined by a sessile drop method using water, glycerol, and diiodomethane as test liquids.[28] First, 1 mL of KL, KL-*g*-AMPS, and PAMPS aqueous solutions with the concentration of 50 g/L were spread on glass slides using a WS-650 spin coater (Laurell Technologies Corp), and then the coated slides were air-dried at room temperature for 24 h and oven-dried at 105 °C for 1 h. The contact angles of the coated slides with test liquids were performed on a Sigma 700 contact angle analyzer (Biolin Scientific Inc., Sweden) using the One Attention software (Biolin Scientific). At least three coated glass slides were prepared for each sample, and their mean values were reported in this paper. The contact angles of alumina with the test liquids were determined using a thin-layer wicking method,[23] which was performed on a Sigma 700 automatic tensiometer (Biolin Scientific Inc., Sweden).

Theoretical Interaction. The extended DLVO, XDLVO, the theory is an accepted approach for the illustration of interfacial forces between two surfaces in colloidal systems.[26] Physicochemical properties, e.g., the contact angle of particles and ζ-potentials of solutions, are closely related to the surface energies of particles. The surface tensions of flocculants (γ_f^{LW}, γ_f^+, γ_f^-) and aluminum oxide particles (γ_a^{LW}, γ_a^+, γ_a^-) can be calculated according to a series of Young's equations with three different liquids (e.g., water, glycerol, and diiodomethane). The surface tensions of these three liquids are found in Table 1. The expression of Young's equation is given in eq 2

$$(1 + \cos\theta)\gamma_l^{TOT} = 2\left(\sqrt{\gamma_s^{LW}\gamma_l^{LW}} + \sqrt{\gamma_s^+\gamma_l^-} + \sqrt{\gamma_l^+\gamma_s^-}\right) \quad (2)$$

where the subscripts l and s represent liquid and solid, respectively. Surface tension (γ^{TOT}) is the sum of an apolar (Lifshitz–van der Waals) (γ^{LW}) and a polar (acid–base) component (γ^{AB}). γ^{AB} includes an electron-donating (γ^-) and an electron-accepting component (γ^+). This set of experiments was conducted for the samples, and the surface tensions of these samples are presented in Table 1.

Table 1. Surface Tension Components (mN/m) of the Liquids Used in the Measurement of Contact Angle[26]

liquids	γ^{LW}	γ^+	γ^-	γ^{AB}	γ^{TOT}
water	21.8	25.5	25.5	51.0	72.8
glycerol	34.0	3.9	57.4	30.0	64.0
diiodomethane	50.8	0.0	0.0	0.0	50.8

In the XDLVO theory, the total interfacial interaction force (ΔG^{TOT}) is the sum of Lifshitz–van der Waals force (ΔG^{LW}), electrostatic force (ΔG^{EL}), and acid–base force (ΔG), as listed in the following equations

$$\Delta G^{TOT}(d) = \Delta G^{LW}(d) + \Delta G^{EL}(d) + \Delta G^{AB}(d) \quad (3)$$

For two interacting spherical particles with radii of a_1 and a_2, $\Delta G^{LW}(d)$, $\Delta G^{EL}(d)$ and $\Delta G^{AB}(d)$ can be expressed as

$$\Delta G^{LW}(d) = -\frac{A(a_1a_2)}{6d(a_1 + a_2)} \quad (4)$$

$$\Delta G^{EL}(d) = \frac{\pi\varepsilon a_1a_2(\xi_1^2 + \xi_2^2)}{6d(a_1 + a_2)}\left[\frac{2\xi_1\xi_2}{\xi_1^2 + \xi_2^2}\ln\frac{1 + e^{-\kappa d}}{1 - e^{-\kappa d}} + \ln(1 - e^{-2\kappa d})\right] \quad (5)$$

$$\Delta G^{AB}(d) = 2\pi\frac{a_1a_2}{(a_1 + a_2)}\lambda\Delta G_{adh}^{AB}\, e^{(d_0 - d)/\lambda} \quad (6)$$

$$A = -12\pi d_0^2\Delta G_{adh}^{LW} \quad (7)$$

where A, ε, ζ, and κ^{-1} are the Hamaker constant, the permittivity of the medium, the ζ-potential, and the double-layer thickness, respectively; λ is the correlation length of the molecule in a liquid medium, 0.6 nm;[27] and d_0 is the distance of the closest approach between two spherical particles, 0.157 nm.[33] ε is usually calculated based on the permittivity of a vacuum (ε_0, 8.854×10^{-12} $C^2/(J\cdot m)$) and the relative permittivity of the medium ε_r, which is 80 for water at 20 °C.[28] κ^{-1} is calculated from eq 8[28]

$$1/\kappa = \left[(\varepsilon kT)/(e^2\sum v_i^2 n_i\right] \quad (8)$$

where k and e are the Boltzmann constant (1.38×10^{-23} J/K) and the charge of an electron (1.602×10^{-19} C), respectively; T is the absolute temperature in K; and v_i and n_i are the valency and the number density (per liter of bulk liquid) of each ionic substance, respectively. In this study, κ^{-1} was calculated to be 9.709 nm.

ΔG_{adh}^{LW} and ΔG_{adh}^{AB} were derived from the Lifshitz–van der Waals/acid–base approach as follows

$$\Delta G_{adh}^{LW} = -2\left(\sqrt{\gamma_a^{LW}} - \sqrt{\gamma_l^{LW}}\right)\left(\sqrt{\gamma_f^{LW}} - \sqrt{\gamma_l^{LW}}\right) \quad (9)$$

$$\Delta G_{adh}^{AB} = +2\left(\sqrt{\gamma_f^+} - \sqrt{\gamma_a^+}\right)\left(\sqrt{\gamma_f^-} - \sqrt{\gamma_a^-}\right) - 2\left(\sqrt{\gamma_f^+} - \sqrt{\gamma_l^+}\right)\left(\sqrt{\gamma_f^-} - \sqrt{\gamma_l^-}\right) - 2\left(\sqrt{\gamma_a^+} - \sqrt{\gamma_l^+}\right)\left(\sqrt{\gamma_a^-} - \sqrt{\gamma_l^-}\right) \quad (10)$$

Flocculation of Aluminum Oxide Suspension. The flocculation affinity of KL-*g*-AMPS, PAMPS, KL, and

https://dx.doi.org/10.1021/acsomega.0c02598
ACS Omega 2020, 5, 21032–21041

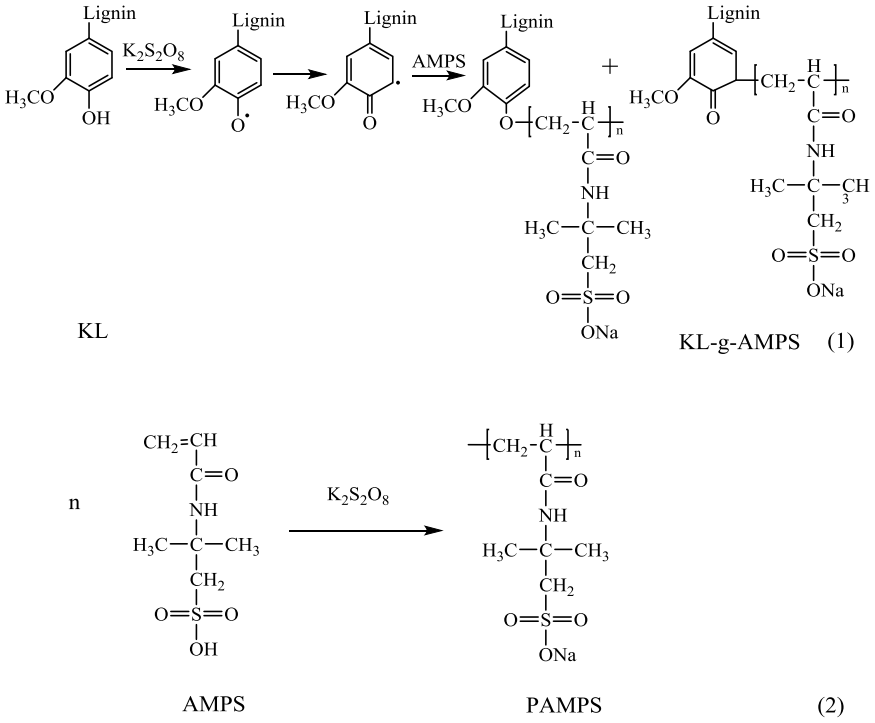

Figure 1. Polymerization of KL and AMPS.

commercial flocculant PAA polymers in aluminum oxide suspension was analyzed on a dynamic drainage jar (DDJ), which was equipped with a photometric dispersion analyzer (PDA 3000, Rank Brothers, U.K.). First, 50 mL of deionized water (pH 7) was added to the DDJ and then the PDA was turned on for 10 min to circulate water at a constant flow rate of 50 mL/min. Second, 50 mL of aluminum oxide suspension (2.5 wt % and pH 7.0) was added into the DDJ at 100 rpm. After reaching a constant state at a flow rate of 50 mL/min, the flocculant solutions (0.5 g/L concentration) were injected into the DDJ. According to eq 11, the relative turbidity was calculated to represent the degree of flocculation from changes in the DC voltages of the PDA analyzer before and after adding flocculants[15]

$$\text{relative turbidity} = \frac{\ln(DC_{H_2O}/DC_f)}{\ln(DC_{H_2O}/DC_i)} \quad (11)$$

where DC_i, DC_f, and DC_{H_2O} are the initial DC voltage of the aluminum oxide suspension before adding flocculants, the final DC voltage of the suspension after adding flocculants, and the initial DC voltage of water solution, respectively.

RESULTS AND DISCUSSION

Graft Polymerization of AMPS onto KL. The reaction of KL and AMPS was carried out in an aqueous solution via free radical polymerization using potassium persulfate as the initiator, which is illustrated in Figure 1. In this reaction, the sulfate-free radicals could be formed by the thermal decomposition of potassium persulfate[34] and were then transferred to either KL or AMPS. Phenoxy radicals on KL were thus generated by accepting the unstable hydrogen from phenolic hydroxyl groups of KL by sulfate radicals,[35] which could also generate resonance radicals. These radicals were then reacted with the AMPS or propagated AMPS to form KL-*g*-AMPS polymer, as depicted in reaction 1 in Figure 1. The AMPS segments in KL-*g*-AMPS polymers contained ionic sulfonate groups and thus offered anionic charges, excellent water solubility, and higher molecular weights to KL. As shown in reaction 2 in Figure 1, AMPS could participate in a side reaction to produce the homopolymer of PAMPS if free radicals were transferred to it. The reaction conditions could influence both lignin-based polymerization and homopolymerization. To minimize side reactions, the reaction conditions were optimized in terms of the charge density and grafting ratio of the desired lignin-based polymer, as stated in the following section.

Reaction Optimization. *pH Effect.* The effect of pH on the charge density and grafting ratio of KL-*g*-AMPS polymer is shown in Figure 2a. It was found that the charge density and grafting ratio of KL-*g*-AMPS polymer decreased with increasing pH value. At pH 1.0, the anionic charge density and grafting ratio were the highest at 4.28 mequiv/g and 325%, respectively. The KL-*g*-AMPS polymer obtained at a pH of 1.5 had a similar charge density and grafting ratio to those obtained at a pH of 1.0. However, when the pH value was higher than 1.5, the grafting ratio and charge density of the polymers were reduced. Therefore, pH 1.5 was selected as the optimum pH. Price and co-workers also reported that the polymerization efficiency of Kraft lignin with dimethyl diallyl ammonium chloride and acrylamide was declined sensibly when the pH value of the reaction medium was higher than 2.0.[35]

Molar Ratio of AMPS/KL. The influence of the AMPS/KL molar ratio on the charge density and grafting ratio of KL-*g*-AMPS polymer is shown in Figure 2b. It was observed that with the increase in the AMPS/KL molar ratio from 0.5:1 to 2.5:1, the anionic charge density and grafting ratio of KL-*g*-AMPS increased from 2.91 meg/g and 41% to 4.27 mequiv/g and 340%, respectively. This result confirmed an increase in the polymerization efficiency of KL and AMPS due to the enhanced AMPS content in the reaction system. However, the

https://dx.doi.org/10.1021/acsomega.0c02598
ACS Omega 2020, 5, 21032−21041

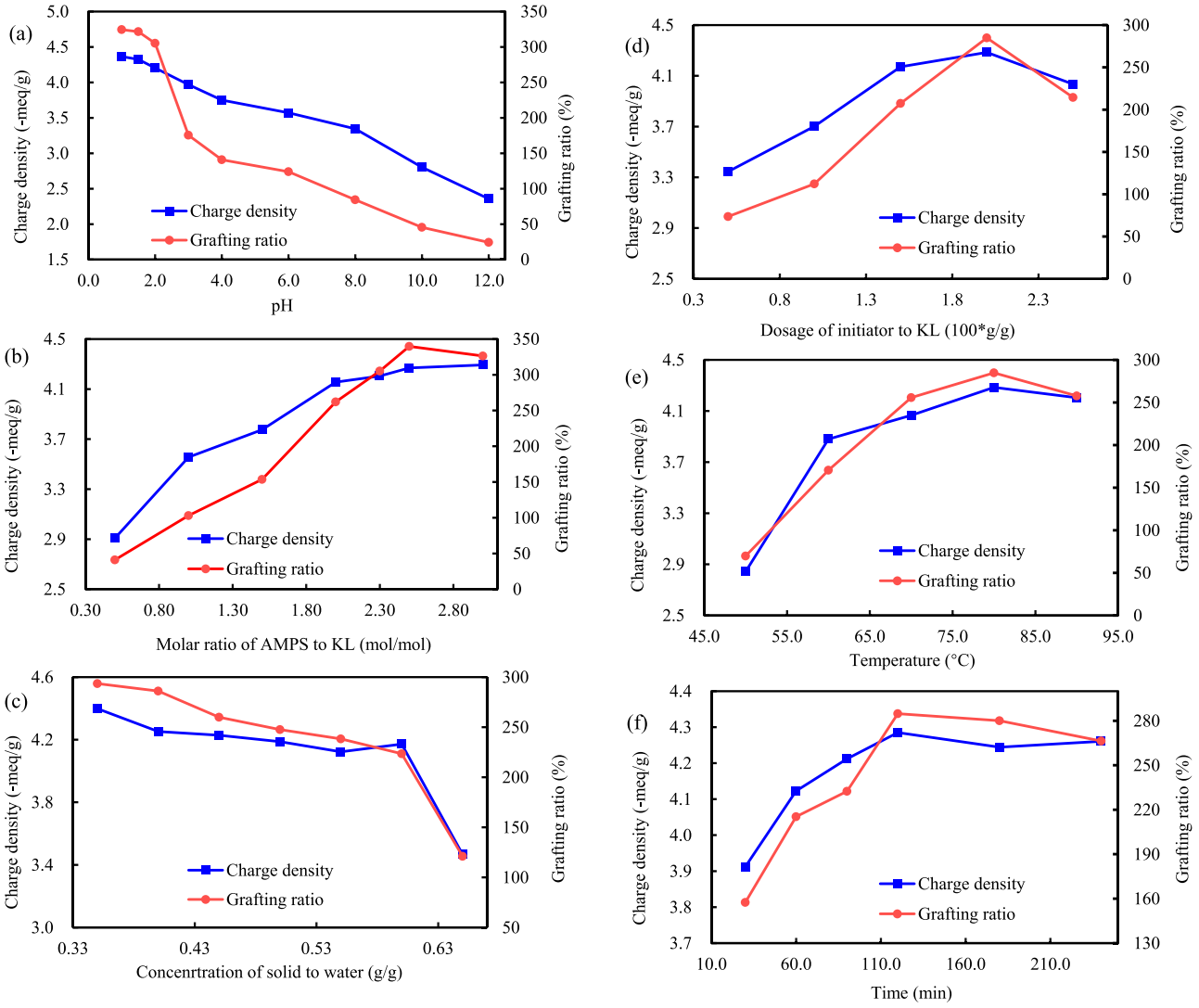

Figure 2. Effects of reaction conditions on the charge density and grafting ratio of KL-*g*-AMPS polymers: (a) pH under the conditions of 2.3 mol/mol AMPS/KL, 0.40 g/g solid/water ratio, 1.5 wt % initiator/KL, 80 °C, 120 min; (b) molar ratio of AMPS/KL under the conditions of 0.40 g/g solid/water ratio, 1.5 wt % initiator/KL, 80 °C, 120 min, pH 1.5; (c) solid/water ratio under the conditions of 2.5 mol/mol AMPS/KL, 1.5 wt % initiator/KL, 80 °C, 120 min, pH 1.5; (d) dosage of initiator under the conditions of 2.5 mol/mol AMPS/KL, 0.60 g/g solid/water ratio, 80 °C, 120 min, pH 1.5; (e) temperature under the conditions of 2.5 mol/mol AMPS/KL, 0.60 g/g solid/water ratio, 2.0 wt % initiator/KL, 120 min, pH 1.5; and (f) time under the conditions of 2.5 mol/mol AMPS/KL, 0.60 g/g solid/water ratio, 2.0 wt % initiator/KL, pH 1.5, 80 °C.

anionic charge density and grafting ratio of KL-*g*-AMPS polymer was reduced when the molar ratio of AMPS/KL was higher than 2.5:1, which could be elucidated by the fact that the homopolymerization of AMPS was probably dominated to generate PAMPS, which hindered the polymerization of KL and AMPS. A similar phenomenon was also found in the polymerization of KL with METAC.[36]

Ratio of Solid/Water. The effect of concentration of solid to water on the charge density and grafting ratio of KL-*g*-AMPS polymer is depicted in Figure 2c. The increase in the ratio of solid/water from 0.30 to 0.60 g/g slightly reduced the anionic charge density and grafting ratio of KL-*g*-AMPS polymer from 4.32 mequiv/g and 286% to 4.17 mequiv/g and 223%, respectively. These reductions in charge density and grafting ratio were ascribed to the fact that the lower contents of the water in the reaction medium could cause the lower mobility of chemical groups, e.g., phenolic hydroxyl radicals in KL, to AMPS[37] and thus decrease the probability of collision among these groups to form KL-*g*-AMPS polymer. When the ratio of solid/water was higher than 0.60 g/g, these two values were dramatically reduced. Therefore, considering the cost of producing polymer and dealing with the potential wastewater generation, the 0.60 g/g ratio of solid/water was selected as the optimized condition.

Dosage of Initiator. The charge density and grafting ratio of KL-*g*-AMPS polymer as a function of initiator dosage are presented in Figure 2d. The anionic charge density of KL-*g*-AMPS polymer increased from 3.35 to 4.28 mequiv/g, when the dosage of initiator/KL elevated from 0.5 to 2.0 wt %. However, further increasing the dosage of initiator/KL from 2.0 to 2.5 wt % could decrease the charge density and grafting ratio of KL-*g*-AMPS. It has been reported that the lower dosage of the initiator led to fewer radicals available for the lignin-based grafting reaction[38] and thus resulted in the polymer with a lower 2-acrylamido-2-methylpropane sulfonic acid (AMPS) content. However, extra radicals would elevate the probability of homopolymerization of AMPS monomer and hamper the chance of APMS reacting with KL. A similar

https://dx.doi.org/10.1021/acsomega.0c02598
ACS Omega 2020, 5, 21032−21041

Table 2. Molecular Weight and Elemental Analysis of KL, PAMPS, KL-*g*-AMPS, and PAA

samples	KL	PAMPS	KL-*g*-AMPS	PAA
M_n (g/mol)	20 400	164 990	145 450	66 000
M_w (g/mol)	43 500	501 920	378 470	408 000
M_w/M_n	2.1	3.0	2.6	6.2
charge density (mequiv/g)	−1.5	−4.4	−4.3	−13.8
grafting ratio (%)			202	
C (%)	59.1	37.3	41.1	
H (%)	5.8	6.4	6.4	
O (%)	26.0	26.9	32.8	
N (%)	0.00	6.0	4.5	
S (%)	2.5	13.4	12.4	
formula	$C_9H_{9.82}O_{2.76}S_{0.13}$	-	$C_9H_{12.06}O_{3.89}N_{0.61}S_{0.73}$	

result was reported for the reaction between KL and acrylic acid.[12]

Temperature. Figure 2e displays the influence of reaction temperature on the charge density and grafting ratio of KL-*g*-AMPS polymer. The anionic charge density and grafting ratio of polymer were enhanced with temperature elevation from 50 to 80 °C, indicating that the polymerization between KL and AMPS was an endothermic reaction, and the increase in the temperature would generate more free radicals and hence a higher polymerization rate. However, when the temperature was raised from 80 to 90 °C, the anionic charge density and grafting ratio of KL-*g*-AMPS polymer decreased from 285% and 4.28 mequiv/g to 258% and 4.20 mequiv/g, respectively. The decrease in the charge density and grafting ratio of KL-*g*-AMPS polymer was ascribed to the fact that more chain termination and transfer reactions took place at a temperature higher than 80 °C. A similar phenomenon was also reported for the preparation of lignin-poly(acrylamide)-poly(2-methacryloyloxyethyl)trimethylammonium chloride[13] and lignin-poly[2-(methacryloyloxy)ethyl]trimethylammonium chloride.[36]

Time. The charge density and grafting ratio of KL-*g*-AMPS polymer as a function of reaction time are depicted in Figure 2f. It was found that both the anionic charge density and the grafting ratios increased with the extending reaction time from 30 to 120 min and reached the highest values of 4.28 mequiv/g and 285%, respectively. This phenomenon was ascribed to the extension of chains in KL-*g*-AMPS polymer and the availability of hydroxyl radicals and AMPS monomer molecules.[12] However, when the time was longer than 120 min, the grafting ratio and charge density of KL-*g*-AMPS polymer was scarcely changed.

Properties of KL-*g*-AMPS and PAMPS. To characterize the polymers, KL-*g*-AMPS derived under the optimized conditions of 2.5 mol/mol AMPS/KL, 0.60 g/g solid/water ratio, 2.0 wt % initiator/KL weight ratio, 80 °C, 120 min, and pH 1.5 was selected as the best sample due to its highest grafting ratio of AMPS on KL-*g*-APMS. The properties of KL-*g*-AMPS, KL, and PAMPS generated under the same conditions are listed in Table 2. The anionic charge density of KL-*g*-AMPS was 4.28 mequiv/g and higher than that of KL (1.5 mequiv/g), which verified the successful grafting of AMPS onto KL. This reported charge density for the lignin polymer was substantially higher than that (3.33 mequiv/g) reported in the previous work on the hydroxypropyl sulfonation of Kraft lignin with 3-chloro-2-hydroxypropansulfonic acid sodium.[39] In terms of the elemental analysis, we found that the oxygen, nitrogen, and sulfur contents of KL-*g*-AMPS were higher, while its carbon content was lower than those of KL. The chemical formulas of KL and KL-*g*-AMPS were $C_9H_{9.82}O_{2.76}S_{0.13}$ and $C_9H_{12.06}O_{3.89}N_{0.61}S_{0.73}$, respectively. According to the nitrogen content, the grafting ratio of KL-*g*-AMPS was calculated to be 285%, which implied that 74 wt % of AMPS and 26 wt % of KL were present in the KL-*g*-AMPS polymer. The average molecular weight of KL-*g*-AMPS was 378 470 g/mol, which was significantly higher than that of KL (43 500 g/mol), demonstrating the successful polymerization of AMPS and KL. Furthermore, the polydispersity of KL was improved after the polymerization. However, the PAMPS prepared under the same reaction conditions had a relatively higher charge density, molecular weight, and polydispersity than that of KL-*g*-AMPS. Based on the nitrogen content, the theoretical charge density of PAMPS was determined to be 4.3 mequiv/g, respectively, which was similar to that of the experimental value (4.4 mequiv/g). It was also found that the charge density and molecular weights of KL-*g*-AMPS were lower than those of PAMPS, which was probably caused by the easier homopolymerization of 2-acrylamide-2-methylpropane sulfonic sodium than polymerization of KL and AMPS in an acidic environment.

^{1}H NMR Analysis of KL, KL-*g*-AMPS, and PAMPS. The ^{1}H NMR spectra of KL, KL-*g*-AMPS, and PAMPS are shown in Figure 3. In the spectra of PAMPS and KL-*g*-AMPS, the peaks for the PAMPS chain segment appeared at 1.39 ppm ($-CH_3$), 1.94 ppm (methylene proton in $-CH_2-CH-$), 3.23 ppm (methyne proton in $-CH_2-CH-$), and 7.34 ppm ($-NH-$). The signal of proton in CH_2-OSO_3 was overlapped

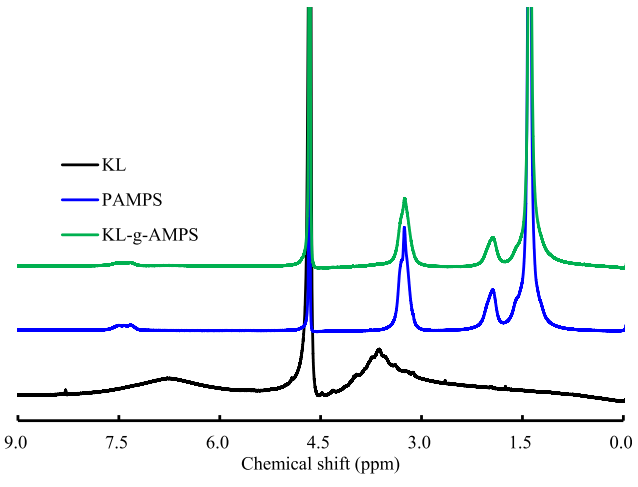

Figure 3. ^{1}H NMR spectra of KL, KL-*g*-AMPS, and PAMPS.

https://dx.doi.org/10.1021/acsomega.0c02598
ACS Omega 2020, 5, 21032−21041

Table 3. ζ-Potentials and Contact Angles of Lignin and KL-g-AMPS Copolymer

	particle size (nm)	ζ-potential (mV)	contact angle (deg)		
			water	diiodomethane	glycerol
KL	18.4 ± 0.6	−22.70 ± 0.83	18.24 ± 0.55	34.81 ± 1.18	46.78 ± 0.23
KL-g-AMPS	158.2 ± 1.3	−52.65 ± 1.14	14.46 ± 0.78	28.30 ± 0.84	44.47 ± 2.10
PAMPS	207.3 ± 4.6	−48.56 ± 1.35	23.84 ± 0.36	43.67 ± 0.99	39.22 ± 2.31
alumina particles	832.3 ± 7.8	+30.06 ± 2.26	64.67 ± 3.42	20.67 ± 1.05	57.21 ± 4.87

by the peak of the solvent. The similar assignments were also reported by Azmeera et al.[18] The characteristic peaks for KL were also found in the spectrum of KL-g-AMPS, which was weak as compared with the peaks for PAMPS. These results confirmed the successful graft polymerization of PAMPS onto KL.

Theoretical Interaction of Flocculants and Particles. Characterization of the surface properties of both aluminum oxide particles and flocculants is necessary for the establishment of the interfacial interaction analysis. The results of the average size and ζ-potential of the aluminum oxide suspensions and flocculants are shown in Table 3. The average size of the KL, KL-g-AMPS, PAMPS, and aluminum oxide were determined to be 18.4, 158.2, 207.3, and 832.3 nm, while their ζ-potentials were −22.7, −52.6, −48.6, and +30.0 mV, respectively. The contact angles of water, glycerol, and diiodomethane on the flocculant coated surfaces are summarized in Table 3.

Based on the results of contact angles, the surface energy components (γ^{LW}, γ^{+}, γ^{-}) of the aluminum oxide particles and the flocculants were calculated using eq 2, and the results are shown in Table 4. With these surface energy components,

Table 4. Surface Energy (mJ/m²) Components of Alumina and Flocculants

samples	γ^{LW}	γ^{+}	γ^{-}
KL	42.12	0.00	64.27
KL-g-AMPS	44.91	0.00	63.83
PAMPS	37.72	0.79	52.20
alumina	47.58	0.17	12.23

ΔG^{LW}_{adh} and ΔG^{AB}_{adh} were separately obtained from eqs 9 and 10, respectively. $\Delta G^{LW}(d)$, $\Delta G^{EL}(d)$, and $\Delta G^{AB}(d)$ were derived using eqs 4−6, respectively. $\Delta G^{TOT}(d)$, the total interaction energy, was calculated by summing the above three energies following eq 3. The plots of these interaction energies versus the separation distance between aluminum oxide and the flocculants are found in Figure 4. It was found that both AB and LW interactions for flocculant and alumina oxide particles were positive, while EL interaction was negative, indicating the AB and LW interactions were repulsive, while the EL interaction was attractive in the flocculation process. ΔG^{TOT} between the flocculants and alumina oxide particles exhibited the secondary minimum due to different strengths and properties of the AB, LW, and EL interactions. In these three interactions, ΔG^{EL} was the dominant force. Hence, it was believed that electrostatic interaction was the primary mechanism for the flocculation process. As shown in the ΔG^{TOT} curves, the secondary minimum depth of PAMPS was slightly larger than that of KL-g-AMPS, and that for both of them were much larger than that of KL. This finding explained the highly efficient flocculation of KL-g-AMPS and PAMPS for

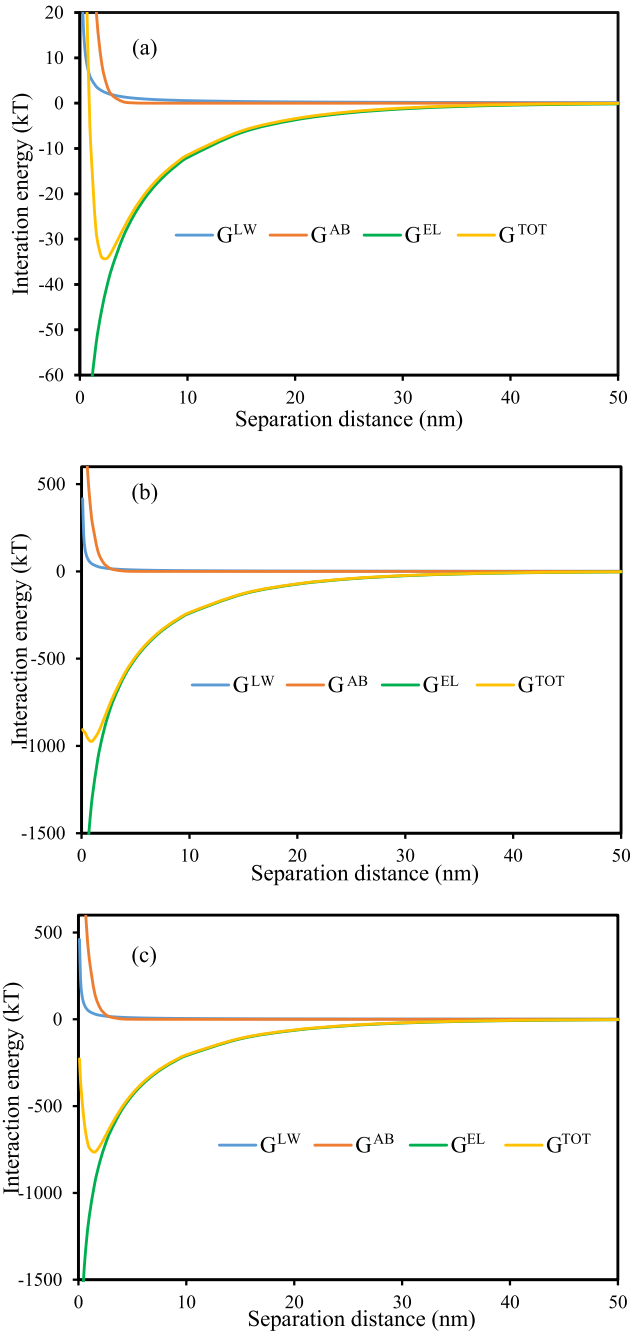

Figure 4. Interaction energies between aluminum oxide particles and flocculants versus the separation distance: (a) KL, (b) PAMPS, and (c) KL-g-AMPS.

aluminum oxide particles, which was in agreement with the results of the flocculation experiment.

As shown in Table 2, the anionic charge density of KL was only 1.5 mequiv/g and much lower than those of KL-g-AMPS

https://dx.doi.org/10.1021/acsomega.0c02598
ACS Omega 2020, 5, 21032−21041

and PAMPS, which endowed a relatively lower ζ-potential. The lower ζ-potential would generate lower EL interaction forces between flocculants and aluminum oxide particles, which was not beneficial for their adhesion and enhancing the flocculation efficiency of aluminum oxide particles. Therefore, to obtain KL-*g*-AMPS flocculant with excellent flocculating ability, the charge density of the polymer may need to be improved.

Flocculation of KL, KL-*g*-AMPS, and PAMPS. The flocculation characteristics of KL, KL-*g*-AMPS, and PAMPS were evaluated in a 0.25 wt % alumina suspension, and the results are presented in Figure 5. The flocculation efficiencies

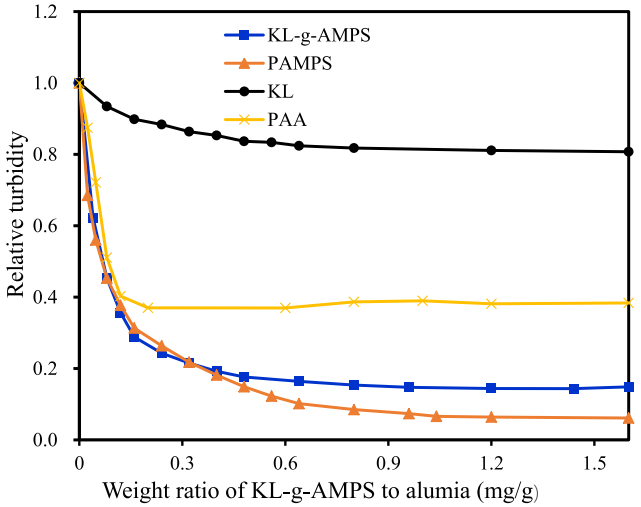

Figure 5. Flocculation performance of KL, KL-*g*-AMPS, and PAMPS in aluminum oxide suspension of 0.25 wt % at pH 7.0.

of KL-*g*-AMPS and PAMPS were elevated with an increase in the dosage of KL-*g*-AMPS and PAMPS in the aluminum oxide suspension. It was well known that flocculation was induced by charge neutralization, bridging, and hydrophobic/hydrophobic interaction.[20,40] The better flocculation efficiency of PAMPS homopolymer than KL-*g*-APAMS was probably attributed to its higher charge density (Table 2). Compared with PAMPS and KL-*g*-AMPS, KL did not flocculate aluminum oxide particles, which was ascribed to the fact that KL had a slightly negative charge density and a very small molecular weight. To achieve the relative turbidity of 0.2, about 0.40 mg/g of KL-*g*-AMPS or PAMPS to alumina was needed. As reported earlier, KL-*g*-AMPS included 74% AMPS and 26% KL. Consequently, it was concluded that 0.30 mg/g of AMPS was required to obtain a 0.2 relative turbidity value when KL-*g*-AMPS was applied. However, to achieve similar relative turbidity, 0.40 mg/g of AMPS was needed when PAMPS was applied. The results indicated that the usage of KL-*g*-AMPS instead of PAMPS would decrease the overall use of AMPS by 25%, which would be important for the development and use of sustainable chemicals. However, AMPS was more effective to achieve a lower relative turbidity (Figure 5), and KL-*g*-AMPS with a higher charge density and molecular weight may be needed to achieve a more efficient flocculant. Considering the advantage of seminatural KL-*g*-AMPS, the polymerization process for the generation of this polymer may be conducted following a different route, e.g., atom transfer radical polymerization (ATRP) polymerization, or KL-*g*-AMPS may be used in a dual flocculation system along with other flocculants.

PAA is a commercial polymer that has extensively been used as a flocculant in industry.[30] The PAA with the molecular weight (M_w) of 408 000 g/mol was selected (Table 2), as it had a molecular weight close to those of KL-*g*-AMPS and PMAPS produced in this study. It can be seen that PAA was less effective in flocculating aluminum oxide particles than other polymers despite their similar molecular weights. As it had a larger polydispersity index than those of other polymers (Table 2), the existence of the low-molecular-weight portion of PAA perhaps did not help with bridging the aluminum oxide particles. Also, the relatively higher charge density of PAA probably prevented its sufficient adsorption on the aluminum oxide particles for flocculating and thus removing aluminum oxide particles.[30,41]

The application of functionalized, negatively charged, and lignin-based polyelectrolytes can be further explored in other colloidal systems. For instance, this anionic polymer, KL-*g*-AMPS, could be a good candidate for the wet end application of papermaking, municipal and industrial wastewater (e.g., pulp and paper), and the removal of various cationic dyes, such as ethyl violet, from the wastewater of the textile industry.[42] Also, KL-*g*-AMPS with a higher charge density (than what was produced in the present research) could potentially be employed as a replacement for lignosulfonate for the removal of sulfur slurry present in the pulp density of the underflow in copper heap leaching process of a mining process.[43]

CONCLUSIONS

The polymerization between KL and AMPS was successfully carried out. The optimal process conditions were 2.5 mol/mol AMPS/lignin, 0.6 g/g solid/water ratio, 2.0 initiator/lignin weight ratio, 80 °C, 120 min, pH 1.5, which yielded KL-*g*-AMPS with the anionic charge density of 4.28 mequiv/g and the grafting ratio of 285%. The ^{1}H NMR and elemental analyses confirmed the successful synthesis of KL-*g*-AMPS polymers. The molecular weight of KL-*g*-APAMS was 378 470 g/mol, while that of KL was 43 500 g/mol. The theoretical analysis revealed the role of short-term interactions in the polymer/particle flocculation system for all polymers. From this analysis, it was discovered that the EL interaction force was the dominant force developed between particles in the flocculation process, indicating that the electrostatic interaction was dominant. To achieve the relative turbidity of 0.2, KL-*g*-AMPS polymers had comparable efficiency with that of PAMPS, indicating that the use of KL-*g*-AMPS would reduce the use of synthetic monomer, AMPS, in flocculating aluminum oxide particles. As PAMS was generally more efficient than KL-*g*-AMPS, to further improve the efficiency of KL-*g*-AMPS, its polymerization reaction may be conducted following a different process or it may be used along with other flocculants in flocculation processes.

AUTHOR INFORMATION

Corresponding Author

Pedram Fatehi − *Department of Chemical Engineering, Lakehead University, Thunder Bay, Ontario P7B5E1, Canada; Key Laboratory of Pulp & Paper Science and Technology, Ministry of Education, Qilu University of Technology, Jinan, Shandong 250353, China;* orcid.org/0000-0002-3874-5089; Email: pfatehi@lakeheadu.ca

https://dx.doi.org/10.1021/acsomega.0c02598
ACS Omega 2020, 5, 21032−21041

Authors

Yanzhu Guo − *Liaoning Key Lab of Pulp and Paper Engineering, Dalian Polytechnic University, Dalian, Liaoning 116034, China; Department of Chemical Engineering, Lakehead University, Thunder Bay, Ontario P7B5E1, Canada*

Fangong Kong − *Key Laboratory of Pulp & Paper Science and Technology, Ministry of Education, Qilu University of Technology, Jinan, Shandong 250353, China;* orcid.org/0000-0003-4230-374X

Complete contact information is available at: https://pubs.acs.org/10.1021/acsomega.0c02598

Author Contributions

Y.G. prepared the manuscript and graphics. F.K. provided scientific support and P.F. was the supervisor and leader of this project. All authors have provided approval for the final version of this manuscript.

Notes

The authors declare no competing financial interest.

■ ACKNOWLEDGMENTS

The authors would like to thank, NSERC Canada, Canada Research Chair, Northern Ontario Heritage Fund Corporation, Canada Foundation for Innovation, LiaoNing Revitalization Talents Program in China (XLYC1807232), and Youth Scientific and Technological Star Project of Dalian City in China (2017RQ036) for supporting this research.

■ REFERENCES

(1) Hafenstine, G. R.; Patalano, R. E.; Harris, A. W.; Jiang, G.; Ma, K.; Goodwin, A. P.; Cha, J. N. Solar Photocatalytic Phenol Polymerization and Hydrogen Generation for Flocculation of Wastewater Impurities. *ACS Appl. Polym. Mater.* **2019**, *1*, 1451−1457.

(2) Tripathy, T.; Karmakar, N. C.; Singh, R. P. Development of Novel Polymeric Flocculant based on Grafted Sodium Aginate for the Treatment of Coal Mine Wastewater. *J. Appl. Polym. Sci.* **2001**, *82*, 375−382.

(3) Lee, K. E.; Morad, N.; Teng, T. T.; Poh, B. T. Development, Characterization and the Application of Hybrid Materials in Coagulation/Flocculation of Wastewater: A Review. *Chem. Eng. J.* **2012**, *203*, 370−386.

(4) Teh, C. Y.; Budiman, P. M.; Shak, K. P. Y.; Wu, T. Y. Recent Advancement of Coagulation-Flocculation and its Application in Wastewater Treatment. *Ind. Eng. Chem. Res.* **2016**, *55*, 4363−4389.

(5) Wu, H.; Liu, Z.; Li, A.; Yang, H. Evaluation of Starch-based Flocculants for the Flocculation of Dissolved Organic Matter from Textile Dyeing Secondary Wastewater. *Chemosphere* **2017**, *174*, 200−207.

(6) Ariffin, A.; Razali, M. A. A.; Ahmad, Z. PolyDADMAC and Polyacrylamide as a Hybrid Flocculation System in the Treatment of Pulp and Paper Mills Wastewater. *Chem. Eng. J.* **2012**, *179*, 107−111.

(7) Suresh, A.; Grygolowicz-Pawlak, E.; Pathak, S.; Poh, L. S.; Abdul Majid, M. B.; Dominiak, D.; Bugge, T. V.; Gao, X.; Ng, W. J. Understanding and Optimization of the Flocculation Process in Biological Wastewater Treatment Processes: A Review. *Chemosphere* **2018**, *210*, 401−416.

(8) Gregory, J.; Barany, S. Adsorption and Flocculation by Polymers and Polymer Mixtures. *Adv. Colloid Interface Sci.* **2011**, *169*, 1−12.

(9) Razali, M. A. A.; Ariffin, A. Polymeric Flocculant based on Cassava Starch Grafted Polydiallyldimethylammonium Chloride: Flocculation Behavior and Mechanism. *Appl. Surf. Sci.* **2015**, *351*, 89−94.

(10) Wang, Y. Y.; Wyman, C. E.; Cai, C. M.; Ragauskas, A. J. Lignin-Based Polyurethanes from Unmodified Kraft Lignin Fractionated by Sequential Precipitation. *ACS Appl. Polym. Mater.* **2019**, *1*, 1672−1679.

(11) Lin, X.; Zhang, J.; Luo, X.; Zhang, C.; Zhou, Y. Removal of Aniline Using Lignin Grafted Acrylic Acid from Aqueous Solution. *Chem. Eng. J.* **2011**, *172*, 856−863.

(12) Kong, F.; Wang, S.; Price, J. T.; Fatehi, P.; Konduri, M. K. R. Water Soluble Kraft Lignin-Acrylic Acid Copolymer: Synthesis and Characterization. *Green Chem.* **2015**, *17*, 4355−4366.

(13) Hasan, A.; Fatehi, P. Synthesis and Characterization of Lignin-poly (acrylamide)-poly (2-methacryloyloxyethyl) trimethyl Ammonium Chloride Copolymer. *J. Appl. Polym. Sci.* **2018**, *135*, No. 46338.

(14) Hasan, A.; Fatehi, P. Cationic Kraft Lignin-Acrylamide Copolymer as a Flocculant for Clay Suspensions:(2) Charge Density Effect. *Sep. Purif. Technol.* **2019**, *210*, 963−972.

(15) Wang, S.; Konduri, M. K. R.; Hou, Q.; Fatehi, P. Cationic Xylan-METAC Copolymer as a Flocculant for Clay Suspensions. *RSC Adv.* **2016**, *6*, 40258−40269.

(16) Cheng, W.; Hu, X.; Wang, D.; Liu, G. H. Preparation and Characteristics of Corn Straw-co-AMPS-co-AA Superabsorbent Hydrogel. *Polymers* **2015**, *7*, 2431−2445.

(17) Yu, J.; Li, Y.; Lu, Q.; Zheng, J.; Yang, S.; Jin, F.; Wang, Q.; Yang, W. Synthesis, Characterization and Adsorption of Cationic Dyes by CS/P (AMPS-co-AM) Hydrogel Initiated by Glow-discharge-electrolysis Plasma. *Iran. Polym. J.* **2016**, *25*, 423−435.

(18) Azmeera, V.; Adhikary, P.; Krishnamoorthi, S. Synthesis and Characterization of Graft Copolymer of Dextran and 2-acrylamido-2-methylpropane Sulphonic Acid. *Int. J. Carbohydr. Chem.* **2012**, *2012*, No. 209085.

(19) Wen, Y.; Wei, B.; Cheng, D.; Ann, X.; Ni, Y. Stability Enhancement of Nanofibrillated Cellulose in Electrolytes through Grafting of 2-acrylamido-2-methylpropane Sulfonic Acid. *Cellulose* **2017**, *24*, 731−738.

(20) Lee, C. S.; Robinson, J.; Chong, M. F. A Review on Application of Flocculants in Wastewater Treatment. *Process Saf. Environ. Prot.* **2014**, *92*, 489−508.

(21) Lu, L.; Pan, Z.; Hao, N.; Peng, W. A Novel Acrylamide-free Flocculant and its Application for Sludge Dewatering. *Water Res.* **2014**, *57*, 304−312.

(22) Kazzaz, A. E.; Feizi, Z. H.; Kong, F.; Fatehi, P. Interaction of Poly (acrylic acid) and Aluminum Oxide Particles in Suspension: Particle Size Effect. *Colloids Surf., A* **2018**, *556*, 218−226.

(23) Nabweteme, R.; Yoo, M.; Kwon, H. S.; Kim, Y. J.; Hwang, G.; Lee, C. H.; Ahn, I. S. Application of the Extended DLVO Approach to Mechanistically Study the Algal Flocculation. *J. Ind. Eng. Chem.* **2015**, *30*, 289−294.

(24) Brenner, H.; O'Neill, M. E. On the Stokes Resistance of Multiparticle Systems in a Linear Shear Field. *Chem. Eng. Sci.* **1972**, *27*, 1421−1439.

(25) Furukawa, Y.; Watkins, J. L. Effect of Organic Matter on the Flocculation of Colloidal Montmorillonite: a Modeling Approach. *J. Coastal Res.* **2012**, *28*, 726−737.

(26) Zhang, M.; Zhou, X.; Shen, L.; Cai, X.; Wang, F.; Chen, J.; Lin, H.; Li, R.; Wu, X.; Liao, B. Q. Quantitative Evaluation of the Interfacial Interactions between a Randomly Rough Sludge Floc and Membrane Surface in a Membrane Bioreactor based on Fractal Geometry. *Bioresour. Technol.* **2017**, *234*, 198−207.

(27) Van Oss, C. J. Aspecific and Specific Intermolecular Interactions in Aqueous Media. *J. Mol. Recognit.* **1990**, *3*, 128−136.

(28) Hwang, G.; Ahn, I. S.; Mhin, B. J.; Kim, J. Y. Adhesion of Nano-sized Particles to the Surface of Bacteria: Mechanistic Study with the Extended DLVO Theory. *Colloids Surf., B* **2012**, *97*, 138−144.

(29) Monfared, A. D.; Ghazanfari, M. H.; Jamialahmadi, M.; Helalizadeh, A. Adsorption of Silica Nanoparticles onto Calcite: Equilibrium, Kinetic, Thermodynamic and DLVO Analysis. *Chem. Eng. J.* **2015**, *281*, 334−344.

(30) Das, K. K.; Somasundaran, P. Flocculation-dispersion characteristics of alumina using a wide molecular weight range of polyacrylic acids. *Colloids Surf., A* **2003**, *223*, 17−25.

(31) Kong, W.; Ren, J.; Wang, S.; Li, M.; Sun, R. C. A Promising Strategy for Preparation of Cationic Xylan by Environment-friendly Semi-dry Oven Process. *Fibers Polym.* **2014**, *15*, 943−949.
(32) Yan, M.; Yang, D.; Deng, Y.; Chen, P.; Zhao, H.; Qiu, X. Influence of pH on the Behavior of Lignosulfonate Macromolecules in Aqueous Solution. *Colloids Surf., A* **2010**, *371*, 50−58.
(33) Van Oss, C. J. Acid-base Interfacial Interactions in Aqueous Media. *Colloids Surf., A* **1993**, *78*, 1−49.
(34) Meister, J. J.; Li, C. T. Synthesis and Properties of Several Cationic Graft Copolymers of Lignin. *Macromolecules* **1992**, *25*, 611−616.
(35) Price, J. T.; Gao, W.; Fatehi, P. Lignin-*g*-poly (acrylamide)-*g*-poly (diallyldimethyl-ammonium chloride): Synthesis, Characterization and Applications. *ChemistryOpen* **2018**, *7*, 645−658.
(36) Wang, S.; Kong, F.; Gao, W.; Fatehi, P. Novel Process for Generating Cationic Lignin based Flocculant. *Ind. Eng. Chem. Res.* **2018**, *57*, 6595−6608.
(37) Heydarifard, S.; Gao, W.; Fatehi, P. Generation of New Cationic Xylan-based Polymer in Industrially Relevant Process. *Ind. Eng. Chem. Res.* **2018**, *57*, 12670−12682.
(38) Shukla, S. R.; Athalye, A. R. Graft-copolymerization of Glycidyl Methacrylate onto Cotton Cellulose. *J. Appl. Polym. Sci.* **1994**, *54*, 279−288.
(39) Guo, Y.; Gao, W.; Fatehi, P. Hydroxypropyl Sulfonated Kraft Lignin as a Coagulant for Cationic Dye. *Ind. Crops Prod.* **2018**, *124*, 273−283.
(40) Shaikh, S. M. R.; Nasser, M. S.; Hussein, I.; Benamor, A.; Onaizi, S. A.; Qiblawey, H. Influence of Polyelectrolytes and other Polymer Complexes on the Flocculation and Rheological Behaviors of Clay Minerals: A Comprehensive Review. *Sep. Purif. Technol.* **2017**, *187*, 137−161.
(41) Zhang, Y.; Gao, W.; Fatehi, P. Structure and settling performance of aluminum oxide and poly(acrylic acid) flocs in suspension systems. *Sep. Purif. Technol.* **2019**, *215*, 115−124.
(42) Bahrpaima, K.; Fatehi, P. Preparation and coagulation performance of carboxypropylated and carboxypentylated lignosulfonates for dye removal. *Biomolecules* **2019**, *9*, No. 383.
(43) Bouffard, S. C.; Tshilombo, A.; West-Sells, P. G. Use of lignosulfonate for elemental sulfur biooxidation and copper leaching. *Miner. Eng.* **2009**, *22*, 100−103.

https://dx.doi.org/10.1021/acsomega.0c02598
ACS Omega 2020, 5, 21032−21041